

NASA Technical Memorandum 4406

Automatic Computation of
Wing-Fuselage Intersection
Lines and Fillet Inserts
With Fixed-Area Constraint

Raymond L. Barger and Mary S. Adams
Langley Research Center
Hampton, Virginia

(NASA-TM-4406) AUTOMATIC
COMPUTATION OF WING-FUSELAGE
INTERSECTION LINES AND FILLET
INSERTS WITH FIXED-AREA CONSTRAINT
(NASA) 19 p

N93-22487

Unclass

H1/02 0153703



National Aeronautics and
Space Administration
Office of Management
Scientific and Technical
Information Program
1993

Abstract

Procedures for automatic computation of wing-fuselage juncture geometry are described. These procedures begin with a geometry in wave-drag format. First, an intersection line is computed by extrapolating the wing to the fuselage. Then two types of filleting procedures are described, both of which utilize a combination of analytical and numerical techniques appropriate for automatic calculation. An analytical technique for estimating the added volume due to the fillet is derived, and an iterative procedure for revising the fuselage to compensate for this additional volume is given. Sample results are included in graphical form.

Introduction

Reference 1 describes methods that are often used for a rapid, approximate analysis of initial "rough cut" supersonic aircraft designs. The methods use a geometry input format of the wave-drag type (ref. 1). The fuselage is input in $x = \text{Constant}$ sections. For the wing, airfoil sections are input at $y = \text{Constant}$ stations in the form of individual camber and thickness distributions.

If the fuselage cross sections are circular, the wave-drag format precludes a smooth fit of the wing to the fuselage. This discrepancy does not cause a problem for the linear analysis codes; however, it does cause one for the application of nonlinear codes, which require a complete surface geometry definition to establish a computational grid. Thus, a system for completing the geometry in the region of the wing-fuselage juncture is required.

Procedures that involve CAD techniques have been developed for this kind of problem and have demonstrated some success in the design of wing-fuselage fillets. However, such hands-on interactive methods are time consuming when geometries are being modified frequently, as in optimal design calculations. Rapid automatic methods are required.

The purpose of this paper is to describe procedures for the automatic treatment of the wing-fuselage juncture problem. First, an intersection line is computed by extrapolating the wing to the fuselage. Then two types of filleting procedures are described. An analytical technique for estimating the added volume due to the fillet is derived, and an iterative procedure for revising the fuselage to compensate for this additional volume is given. Finally, sample results are presented in graphical form.

Although the filleting procedure was developed for supersonic-type configurations, it should be adaptable to lower speed designs as well. The analysis is restricted to configurations with circular-cross-section fuselages, but the techniques can be extended to

more general configurations with a slight increase in complexity. Also, similar methods can be applied to fuselage-fin intersections, wing-pylon intersections, etc.

Symbols

A	area
A_{net}	net area (eq. (14))
A_{pol}	area of polygon
A_{sect}	area of sector of circle
A_{wr}	area of wing cross section included in polygon
\mathbf{a}_i	vector coefficients in equation (7)
\mathbf{c}	vector location of generic point on camber line
$c(x)$	z -coordinate of camber line as a continuous function of x
$d(t)$	absolute distance (eq. (5))
$e(t)$	error indicating extent to which \mathbf{v} is displaced from fuselage surface
\mathbf{f}	vector location of point on fillet surface
\mathbf{f}_t	vector location of point on fillet surface in transition region
$\hat{i}, \hat{j}, \hat{k}$	orthonormal base vectors
L	nondimensional distance defined by equation (8)
l_b	blending distance
\mathbf{r}	vector location of generic point on fuselage surface
$r(x)$	fuselage radius as a continuous function of x

s	nondimensional y -coordinate along fillet line, starting at initial point on fuselage
t	parameter controlling length of \mathbf{v} (eq. (4))
\mathbf{v}	variable-length vector defined by equation (4)
v_x	x -component of \mathbf{v}
\mathbf{w}	position vector of point on wing-upper-surface lofting line at airfoil section location
x, y, z	Cartesian coordinates
x_{le}	value of x at leading edge
θ	angular coordinate
θ_u	angular distance along fuselage allowed for filleting
θ_w	θ -location of intersection of wing leading edge with fuselage
λ	blending function defined by equation (9)
$\rho(x)$	fillet radius for circular-arc fillet

Procedure

Wing-Fuselage Intersection

In the wave-drag format, a wing is defined by individual airfoil sections at specified span stations (fig. 1(a)). A single table of percent locations determines the x -locations at which values of camber and thickness are input. Points on the upper surface are determined by adding the semithickness to the camber coordinate at each location; similarly, the lower surface is obtained by subtracting the semithickness from the camber coordinate. A spanwise line that connects the surface points at a given percent chord location is called a wing lofting line (fig. 1(b)).

The fuselage is entered as a set of circles at specified x -stations, centered at points determined by the fuselage camber line coordinates at these x -stations. Since camber ordinates can be interpolated at any x -location from the camber line array, the camber line shape can be defined by a function $c(x)$ which is determined by these interpolated values. Similarly, a radius distribution $r(x)$ can be synthesized from the input array of fuselage radii. The following surface equation for the fuselage can then be written:

$$\mathbf{r}(x, \theta) = x\hat{i} + y\hat{j} + z\hat{k} \quad (1)$$

where

$$y(x, \theta) = r(x) \cos \theta \quad (2)$$

and

$$z(x, \theta) = c(x) + r(x) \sin \theta \quad (3)$$

To extrapolate the wing lofting lines inward to the fuselage, begin on the upper surface, let \mathbf{w}_1 be the vector location of a point on the first airfoil section (i.e., the most inboard section), and let \mathbf{w}_2 be the location of the corresponding point on the second airfoil section. Thus, \mathbf{w}_1 and \mathbf{w}_2 lie on the same lofting line. A variable-length vector that is collinear with these two points and pointing inward toward the fuselage is

$$\mathbf{v} = \mathbf{w}_1 + t(\mathbf{w}_1 - \mathbf{w}_2) \quad (4)$$

where t is a small but otherwise arbitrary number. If the x -coordinate of $\mathbf{v}(t)$ is denoted v_x and the vector location of the camber line at $v_x(t)$ is denoted $\mathbf{c}(t)$, then the distance from $\mathbf{c}(t)$ to $\mathbf{v}(t)$ is (see fig. 2)

$$d(t) = |\mathbf{v}(t) - \mathbf{c}(t)| \quad (5)$$

Compare this distance with the fuselage radius $r(v_x)$ at v_x to find the error e :

$$e(t) = d(t) - r[v_x(t)] \quad (6)$$

Now the value of t in equation (4) is incremented by an amount that is proportional to $e(t)$, and the procedure is iterated until $e(t)$ is below a specified bound. The components of \mathbf{v} are then taken as a point on the wing-fuselage intersection line.

Figure 3 shows an intersection line computed in this manner. Figure 3(a) shows a planform view computed from the original wave-drag format data and displays the wing-fuselage gap. Figure 3(b) shows the upper surface with the wing extended to the intersection line.

For the intersection of the wing lower surface with the fuselage, a similar procedure is followed. However, the intersection points generally will occur at different x -locations from those of the upper surface. If the fuselage is to be described as a single network, this difference is inconvenient for purposes of surface gridding. Therefore, a new set of intersection points is determined at the same x -locations as the upper-surface intersection points by interpolation in the initial set of lower-surface intersection points. Now, in general, each of these new points is no longer collinear with the corresponding points on the first and second airfoil sections. This effect is apparent in figure 4, which displays the lower-surface intersection

line and the wing lofting lines for the same configuration shown in figure 3. This complication does not arise if the fuselage is not required to be described as a single network, because, in that case, the lower-surface intersection points are computed and used in exactly the same manner as those for the upper surface.

Output Format and Surface Grid Considerations

The output geometry can be expressed in a Hess format (ref. 2). The wing upper and lower surfaces are written as separate networks. The wing-fuselage intersection line is the first Hess format n -line, and the subsequent n -lines are the surface coordinates of the input airfoil sections. The Hess format m -lines are the wing lofting lines. They connect corresponding points (points at the same percent chord locations) on the n -lines. To calculate surface grids, one can interpolate arbitrarily in this network of m - and n -lines.

For the fuselage, the n -lines are circles centered on the camber line. The coordinates are printed at constant values of θ ahead and aft of the wing region. However, if the fuselage is to be described as a single network and this system is used in the wing region, some fuselage network points will fall within the wing-fuselage juncture. To avoid this problem, redistribute the fuselage points in the following manner. Determine θ_w , the θ -location of the intersection of the wing leading edge with the fuselage. The difference between θ_w and -90° is proportional to the arc length along the fuselage from the -90° (vertical downward) location to the wing-leading-edge intersection point. Use the ratio of this arc length to the full semicircle arc length to determine that fraction of the total number of fuselage points that will be assigned below the wing. Locate these points at equal arc locations from the -90° point to the wing-root lower surface. The remaining points are similarly located at equal arc locations above the wing-fuselage intersection. The result is a slight shearing (skewing) of the fuselage grid lines near the wing leading edge, as shown in figure 5. This example was computed for a wing that was set well below the fuselage mid-section. Again, some of these complications do not arise if the part of the fuselage in the wing region is described in separate upper- and lower-surface blocks and not as part of a single fuselage network.

Cubic-Arc Filleting Procedure

If a fillet is required in the wing-fuselage juncture, the fillet design begins with the calculation of wing-fuselage intersection points that was described above.

Then a fuselage n -line is interpolated through each of these intersection points. The following procedure is used for computing the upper-surface fillet lines, except in regions near the leading and trailing edges, where special treatment is required. Starting at the wing-fuselage intersection point and moving up the circular fuselage cross section a preassigned angular distance θ_u , mark the beginning point of the fillet line (fig. 6). Next, determine the end location of the fillet line on the corresponding wing lofting line. This location can optionally be assigned either at a fraction of the distance from the first to the second airfoil section, at a fraction of the distance from the intersection point to the second airfoil section, or at a specified y -increment from the intersection point. Finally, the fillet line is prescribed as a cubic arc (in three-dimensional space) that is tangent to the fuselage circle at the beginning point and to the wing lofting line at the end point. Thus, a point on the fillet is located by the vector

$$\mathbf{f} = \mathbf{a}_1 + \mathbf{a}_2s + \mathbf{a}_3s^2 + \mathbf{a}_4s^3 \quad (7)$$

where s is the nondimensional y -coordinate along the fillet line and the \mathbf{a}_i are vector coefficients determined by the four end conditions.

This procedure cannot be applied without modification near the wing leading and trailing edges, as such an application would lead to problems, such as an effective blunting of the wing near the root. Furthermore, the wing leading edge generally should not be faired tangent to the fuselage, as a change in the leading-edge sweep would be required. Therefore, the adopted scheme leaves the intersection point unchanged at the leading edge. Then, the cubic-arc filleting is blended in gradually over a preassigned distance. Let this blending occur over a distance l_b in the x -direction. Then one can define a nondimensional distance

$$L = \frac{x - x_{le}}{l_b} \quad (8)$$

and a blending function $\lambda(L)$ that varies monotonically from 0 to 1 with L . An appropriate blending function in this procedure is, for example,

$$\lambda(L) = \sin\left(\frac{\pi}{2}L\right) \quad (9)$$

If \mathbf{v} denotes a point on the extrapolated lofting line (eq. (4)) and \mathbf{f} denotes the corresponding point on the fillet arc (eq. (7)), then over the transition distance l_b the fillet is described by the quantity

$$\mathbf{f}_t = [1 - \lambda(L)]\mathbf{v} + \lambda(L)\mathbf{f} \quad (10)$$

A similar procedure is applied near the trailing edge. Then, the entire procedure is applied to the wing lower surface.

Figure 7 gives an example of filleting computed in this manner. The results for the upper surface are shown in figure 7(a), where the transition from a sharp intersection at the leading edge to a curved fillet is apparent. Figure 7(b) shows the lower-surface filleting.

Special situations. A problem can arise when fillet arcs are described by cubic curves if the wing is set very low on the fuselage so that the angle between the extrapolated wing surface and the fuselage is highly acute. In this case, the z -coordinates of the upper-surface fillet arc may dip below the level of the extrapolated wing surface and thereby cause an unacceptable thinning of the wing in this region. One solution to this problem is to increase the fillet angular distance θ_u . A second possibility is to apply a constraint to the z -coordinates of the fillet lines. However, this alternative may lead to slope discontinuities in the fillet line. A third approach is to use the method of blended parabolas. A fourth technique is to forego a polynomial fit to the configuration construction lines and utilize a circular-arc fillet as described below.

Another type of problem arises when an extrapolated lower-surface lofting line fails to intersect the fuselage surface. In this case the $\theta = -90^\circ$ location at the appropriate x -station is taken as the initial point for the fillet line, and the initial values of both $\frac{dx}{dy}$ and $\frac{dz}{dy}$ are set equal to 0 to maintain first-derivative continuity.

Circular-arc filleting. As mentioned above, one alternate procedure is to specify a wing-fuselage fillet as a circular arc of given radius at constant x -stations. The method that is described here to compute these circular arcs is appropriate in the context of the goal of this analysis. The calculation is initiated at a point on a wing lofting line at or near the second airfoil section. Compute the direction vector of the lofting line at this point. Then, take the component of this vector in the $x = \text{Constant}$ plane at this point. In this plane, construct the normal to this vector component (fig. 8(a)) and mark the distance $\rho(x)$ along the normal. Compute the distance from this point to the center of the fuselage as in equation (5), where $\mathbf{v}(t)$ has been replaced by the vector location of the point on the normal to the lofting line direction vector component. Then an error is computed as in equation (6), where the

radius \mathbf{r} is now replaced by an augmented radius $\mathbf{r}(x) + \rho(x)$. Now, return to the original lofting line and take an incremental step inward, as was done to compute the wing-fuselage intersection points. At this new location, the values of $x, y, z, \mathbf{r}(x)$, and $\rho(x)$ are different from those at the previous point. The previous calculation is repeated at this location to yield a smaller error. The process is iterated, taking increments proportional to the error until the error is reduced below a specified bound. Now, the point on the normal to the projected lofting line is a distance $\rho(x)$ from the projected lofting line and also from the fuselage cross section (fig. 8(b)). A circular arc, centered at this point with radius $\rho(x)$, will be tangent to both lines. Thus, a grid line that includes the fuselage circular arc, the fillet circular arc, and the wing lofting line from the point of tangency is continuous. At the fuselage-fillet juncture, the first derivatives are continuous. At the juncture of the fillet and the lofting line, the derivatives of y and z with respect to arc distance are continuous, but the derivative of x is discontinuous. Figure 9 shows an example of a fillet computed in this manner.

Output and Surface Grid Considerations

The surface geometry can be output in four blocks (networks). The first and fourth consist of fuselage coordinates ahead and aft of the wing section, respectively. The second block represents the configuration upper surface in the wing region (fig. 7(a)). Each n -line begins with the grid points on the circular-arc fuselage section, then encompasses points along the fillet line, and finally points along the wing lofting line at the prescribed airfoil locations (excluding the first section, which has been replaced by the fillet). The third block of grid points is computed similarly from the lower-surface geometry.

Another output option is to separate the fuselage in the wing region and the wing into different blocks. The surface would then consist of six output blocks.

Redesign To Compensate for Added Volume

The zero-lift wave drag of a configuration is highly sensitive to the manner in which the volume is distributed. Consequently, the addition of volume due to the fillet can result in an increase in drag because the original configuration presumably already represents an optimal low-drag design.

A simple approach to modifying the geometry to compensate for the added volume is to reduce the fuselage radius distribution in an appropriate manner. However, there is some question as to what

constitutes the most appropriate manner. If the configuration is quite slender, its wave drag can be estimated by the Eminton-Lord formula (ref. 3), which computes the drag from the longitudinal distribution of cross-sectional areas and is independent of Mach number. For practical configurations, a more accurate estimate can be obtained by the use of the Hayes linear supersonic theory (ref. 4). This method employs equivalent area distributions obtained from several sets of Mach plane slices through the configuration. A drag value is computed from each area distribution, and the individual drag values are averaged to obtain the total configuration wave drag. If the fuselage were redesigned to allow for the fillet cross-sectional area by projecting this area along Mach planes, the x -displacement would be slight because the area is added in an inboard region. In addition, this x -displacement would be ambiguous because it would be different for different Mach slice angles.

The actual method adopted to compute the added area due to the fillet was to project an upper-surface fillet line into an $x = \text{Constant}$ plane, together with the corresponding lower-surface line, and to compute the area of the corresponding two-dimensional figure (fig. 10). For the example shown in figure 10, five points were taken on the upper-surface line—one at the beginning (fuselage end), and one at the end, and three at intermediate grid locations. The five points on the lower-surface line correspond to those on the upper surface. The area of the polygon formed by connecting these 10 points is computed by the well-known formula:

$$A_{\text{pol}} = \frac{1}{2} \sum_{i=1}^n (y_i z_{i+1} - z_i y_{i+1}) \quad (11)$$

where $(y_{n+1}, z_{n+1}) = (y_1, z_1)$ and $x = \text{Constant}$. In this case $n = 10$. From this polygon area, one must subtract the included area of the wing root

$$A_{\text{wr}} = \frac{1}{2} (y_5 - y_a) (z_5 - z_6 + z_a - z_b) \quad (12)$$

and the included sector area

$$A_{\text{sect}} = \frac{r^2}{2} (\theta_{\text{sub}} - \sin \theta_{\text{sub}}) \quad (13)$$

where θ_{sub} is the angle subtended by the arc of the sector. The net added area is

$$A_{\text{net}} = A_{\text{pol}} - A_{\text{wr}} - A_{\text{sect}} \quad (14)$$

The fuselage radius is decreased to reduce the fuselage cross-sectional area by just this amount. Then the procedure is iterated until the sum of the fuselage cross-sectional area and the added area from equation (14) approximate the value of the initial fuselage cross-sectional area within a specified error bound.

It is worth noting that the area increment that results from filleting is potentially greater for a low- or high-mounted wing than for a mid-mounted wing. If the initial airfoil section is set close to the fuselage at midsection, the area of the gap is small (fig. 11(a)). However, if the wing is mounted low on the fuselage, the gap is necessarily larger (fig. 11(b)).

A larger gap also occurs when the fuselage has a considerable "wasping" due to area ruling. In this case, the gap may be small where the fuselage radius is a maximum, but greater where the radius has been reduced by area ruling. This larger gap requires more area for filleting, and consequently, an even greater compensating reduction in the fuselage radius.

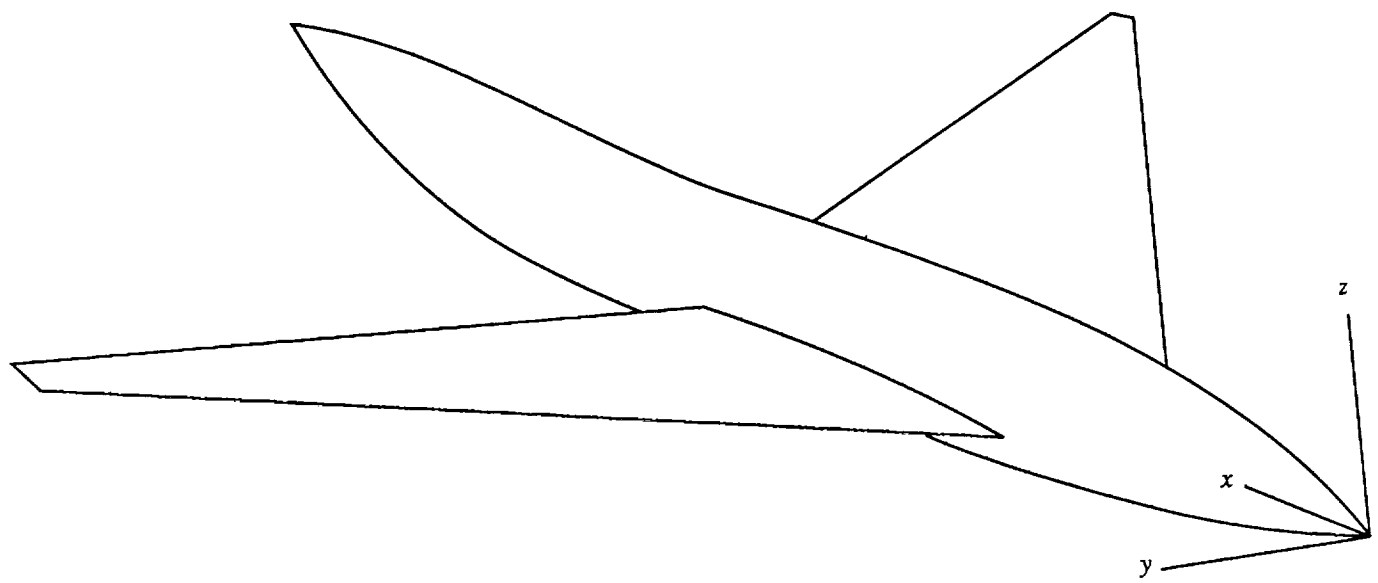
Concluding Remarks

Procedures for automatic computation of wing-fuselage juncture geometry have been described. First, a system was described for computing the intersection line by extrapolating the wing to the fuselage. Then two types of filleting procedures were explained. An analytical technique for estimating the added volume due to the fillet was derived, and an iterative procedure for revising the fuselage to compensate for this additional volume was given. Sample results were included in graphical form.

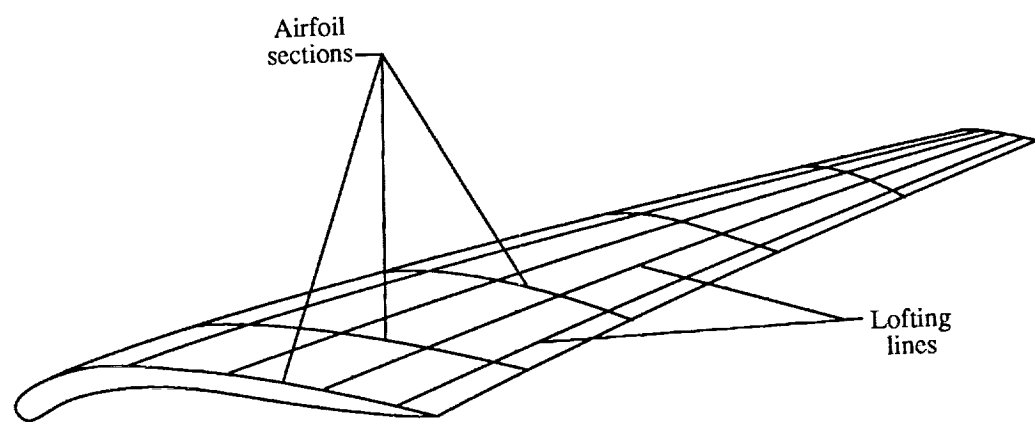
NASA Langley Research Center
Hampton, VA 23681-0001
November 9, 1992

References

1. Craibon, Charlotte B.: *User's Guide for a Computer Program for Calculating the Zero-Lift Wave Drag of Complex Aircraft Configurations*. NASA TM-85670, 1983.
2. Halsey, N. D.; and Hess, J. L.: *A Geometry Package for Generation of Input Data for a Three-Dimensional Potential-Flow Program*. NASA CR-2962, 1978.
3. Eminton, E.; and Lord, W. T.: Note on the Numerical Evaluation of the Wave Drag of Smooth Slender Bodies Using Optimum Area Distributions for Minimum Wave Drag. *J. Royal Aeronaut. Soc.*, vol. 60, no. 541, Jan. 1956, pp. 61-63.
4. Jones, Robert T.: *Theory of Wing-Body Drag at Supersonic Speeds*. NACA Rep. 1284, 1956. (Supersedes NACA RM A53H18a.)



(a) Coordinate system.



(b) Wing geometry.

Figure 1. Coordinate system and basic wing geometry.

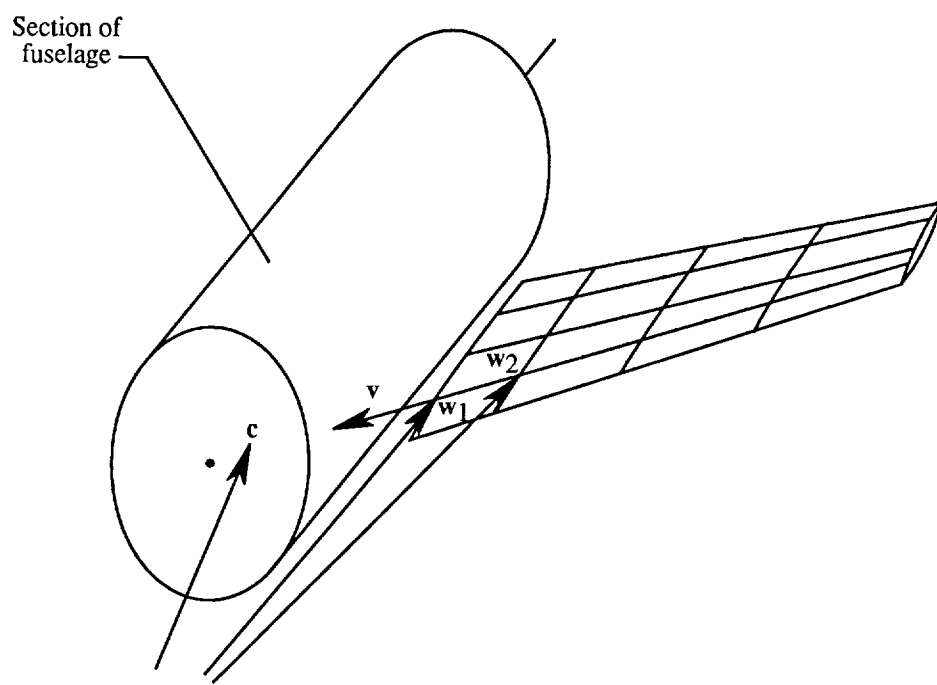
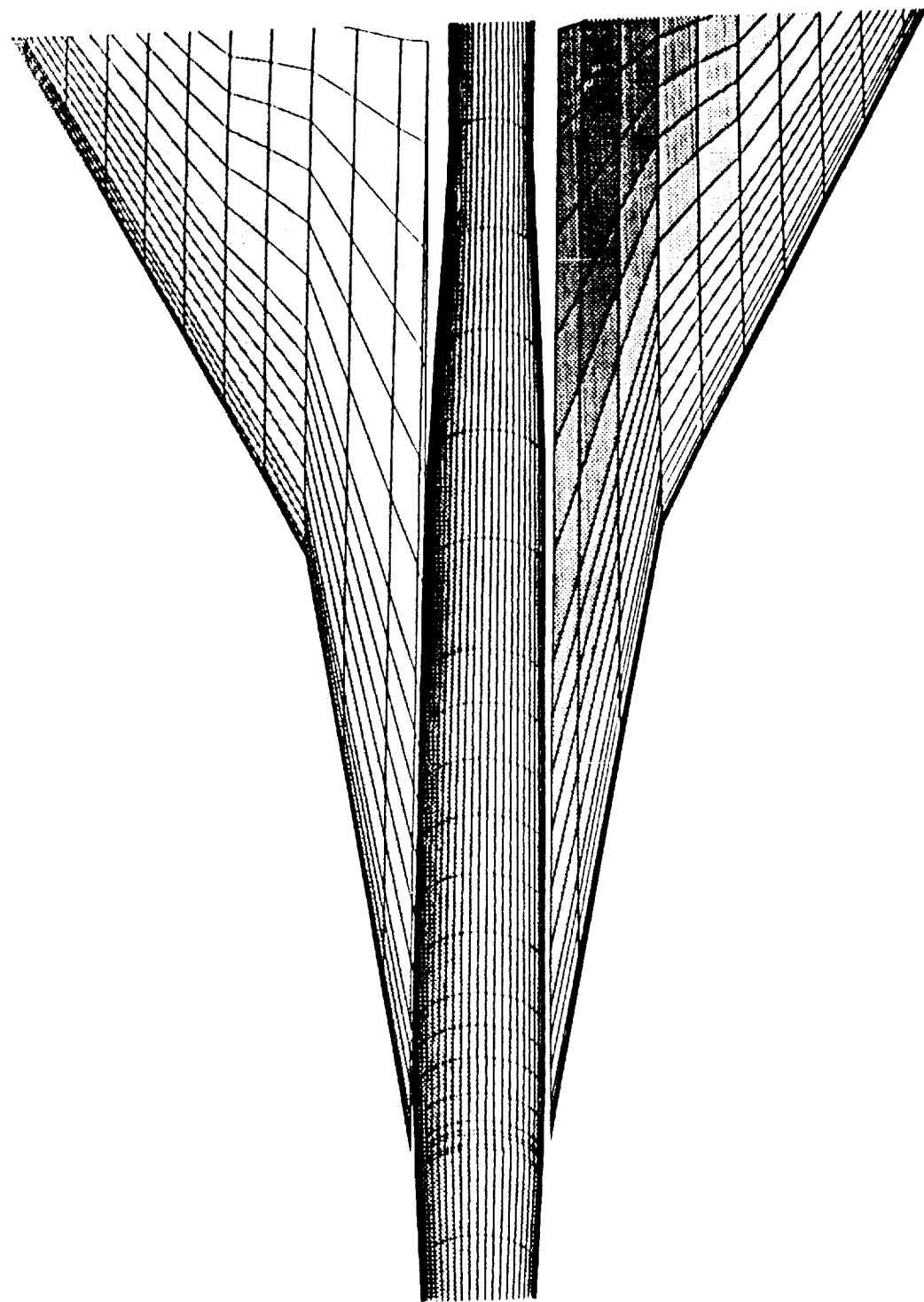
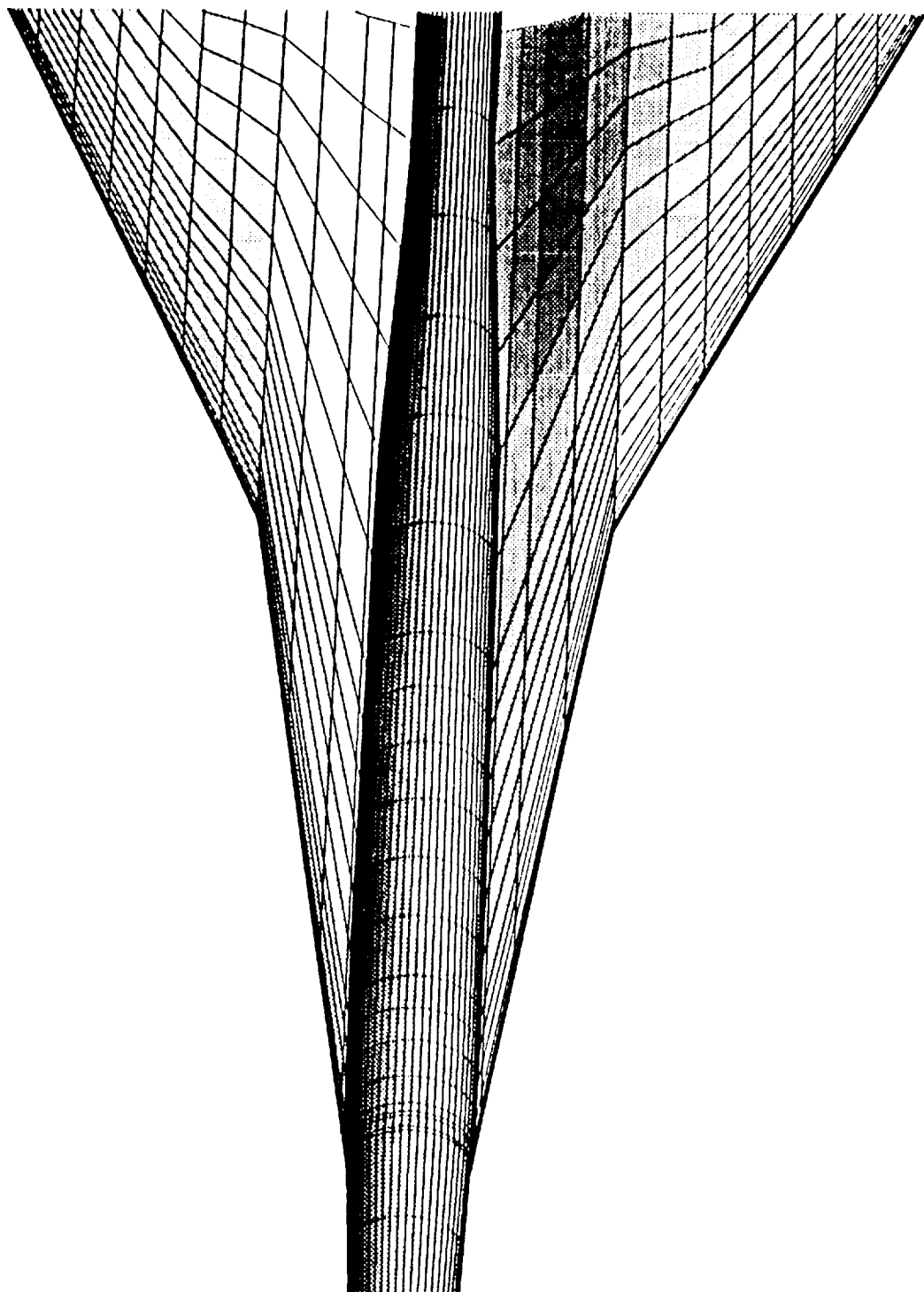


Figure 2. Extrapolation of wing lofting line toward fuselage.



(a) Original configuration (from wave-drag data).

Figure 3. Example of calculated wing-fuselage intersection.



(b) Configuration with computed intersection line.

Figure 3. Concluded.

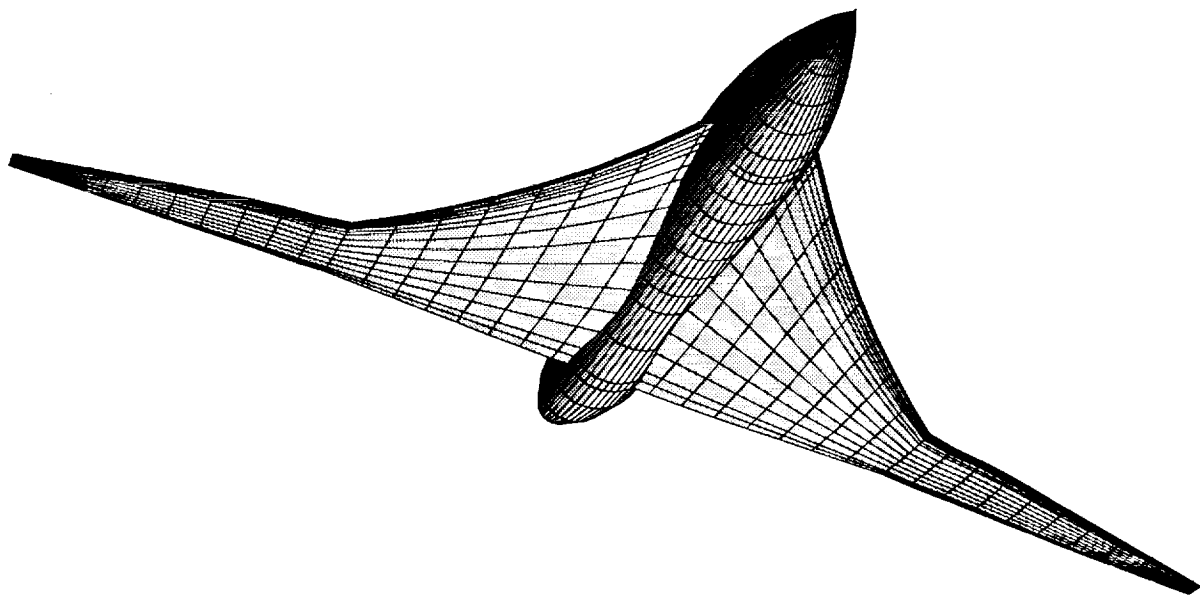


Figure 4. Lower-surface intersection line for configuration in figure 3.

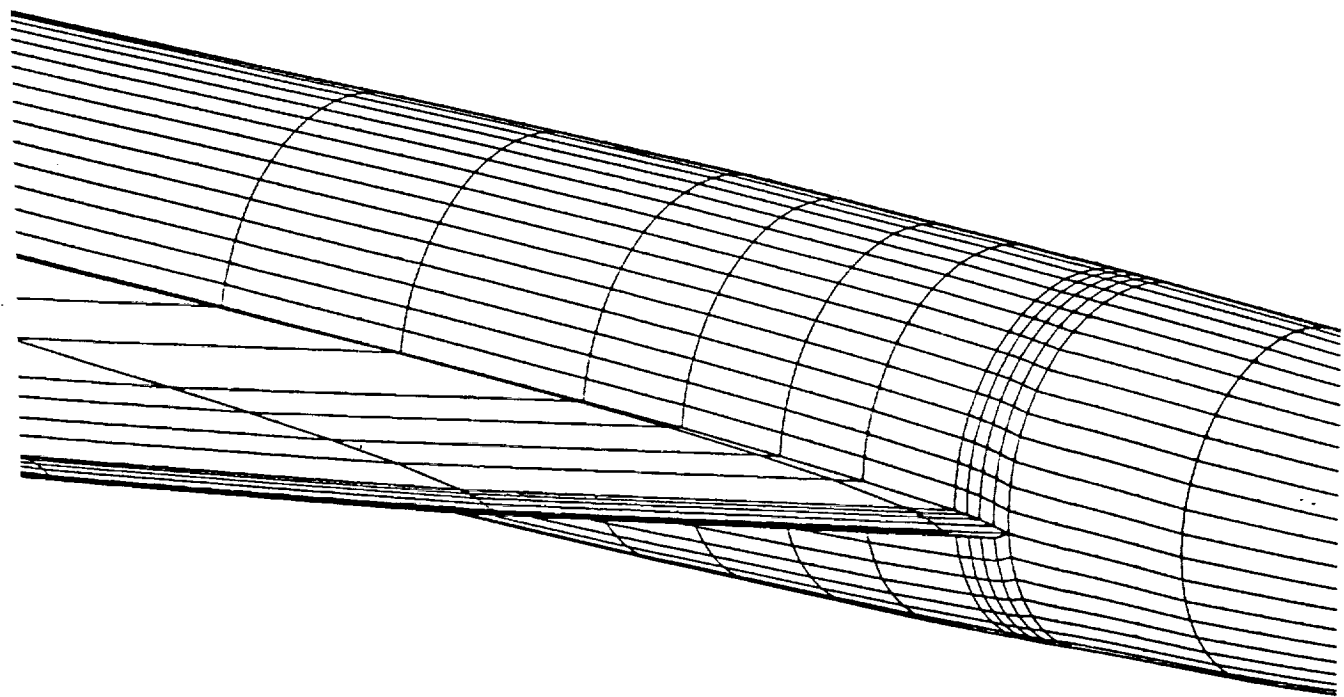


Figure 5. Close-up view of intersection line and surface grid near wing leading edge.

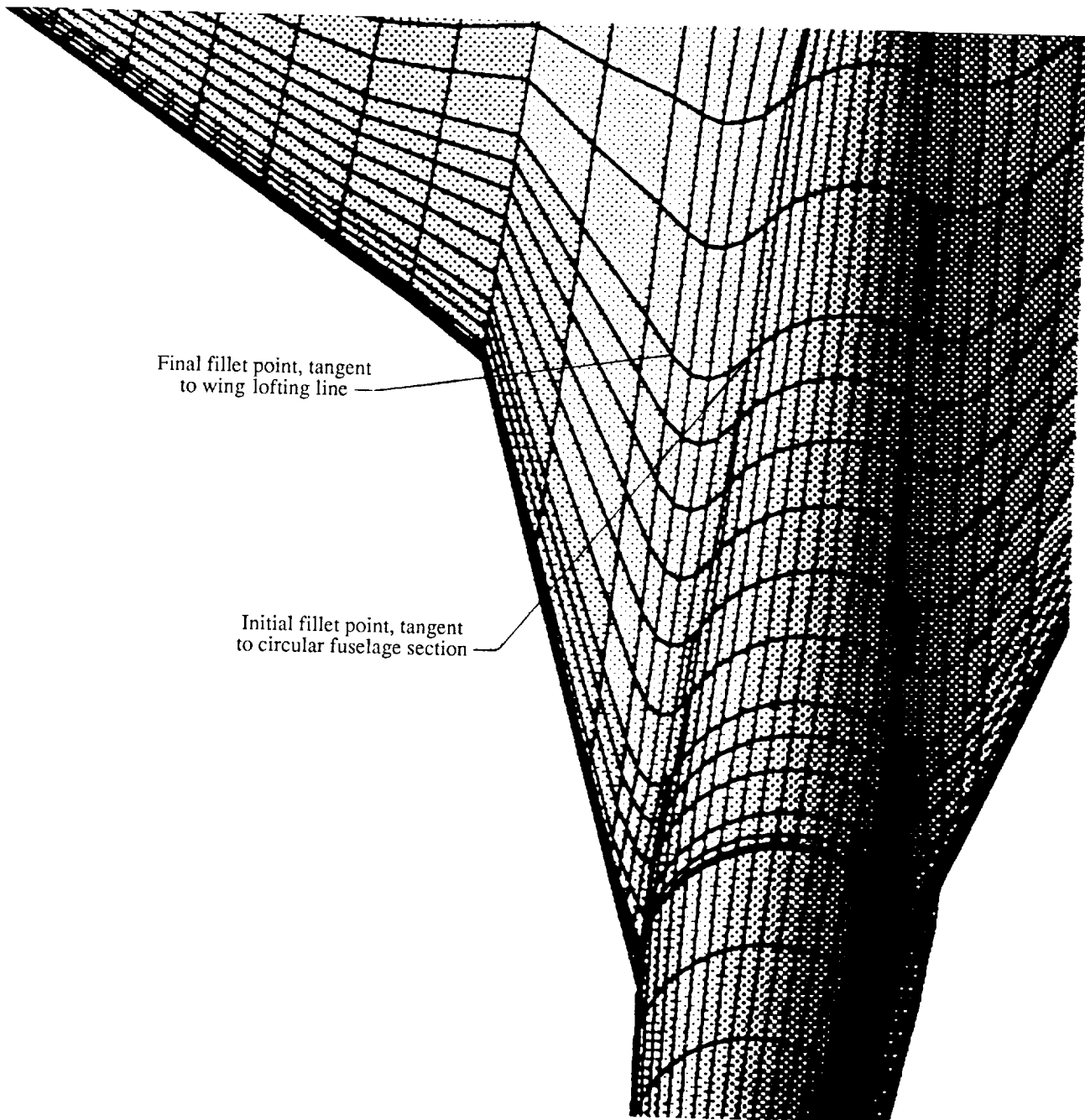
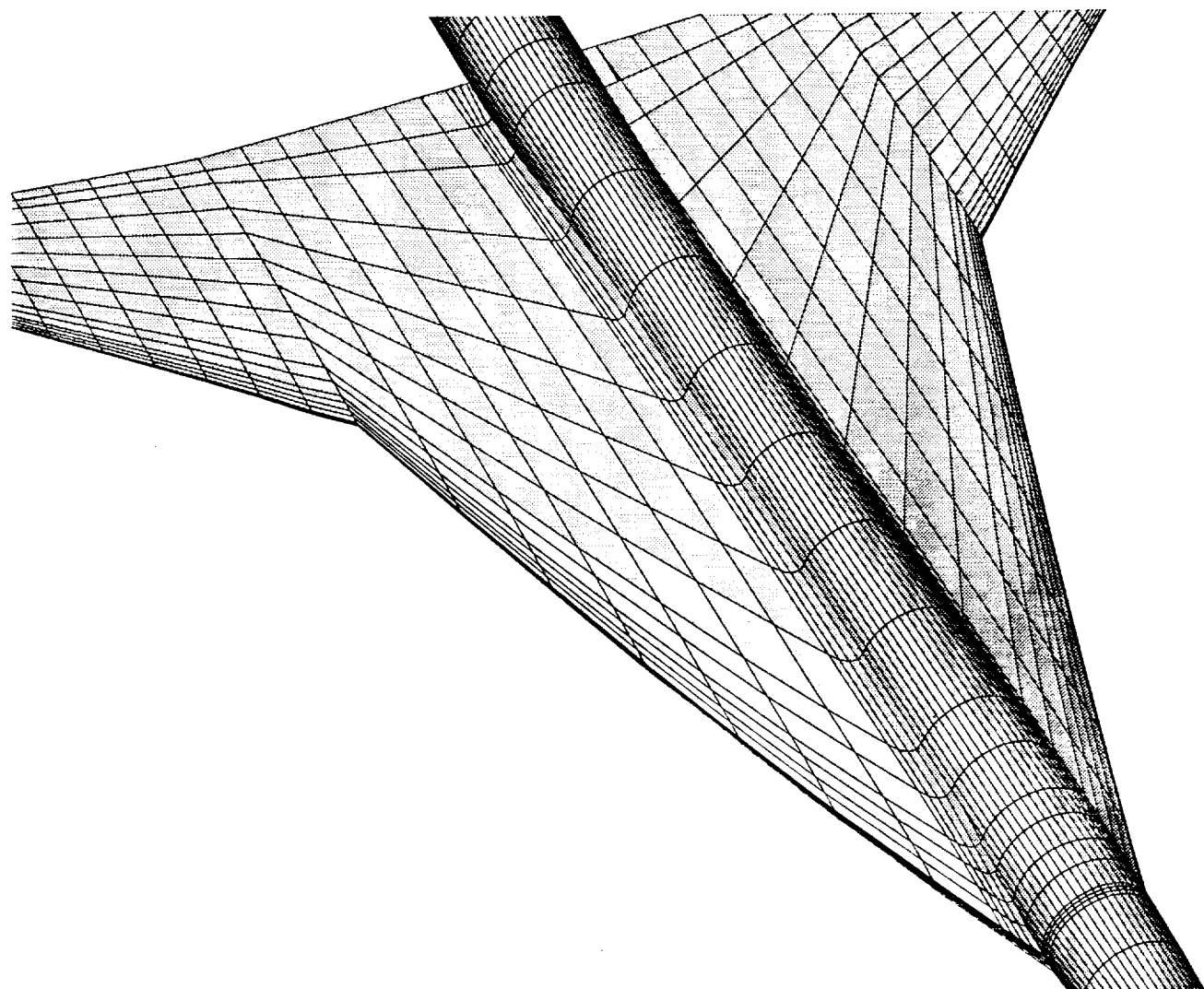
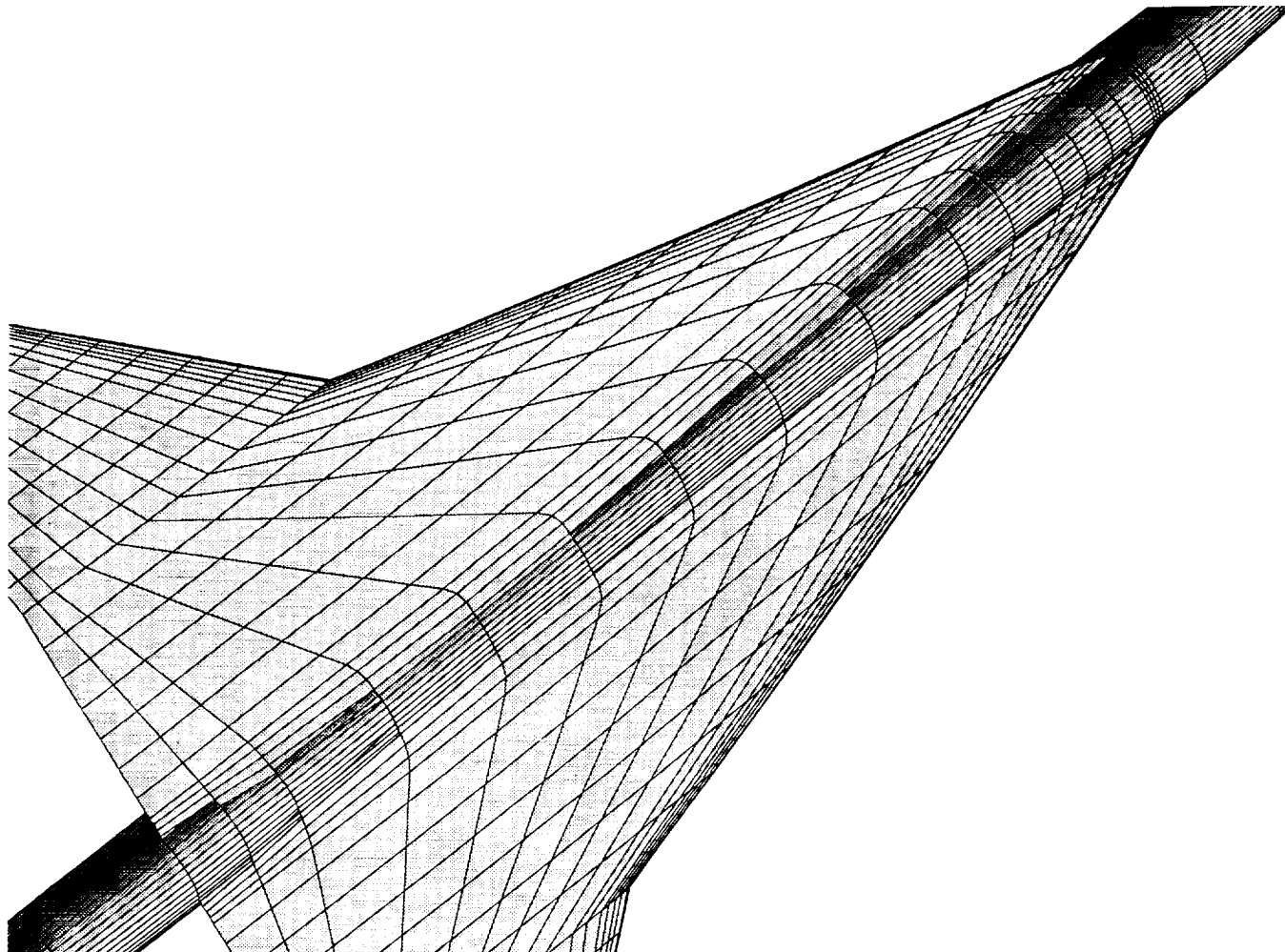


Figure 6. System for inserting fillet line.



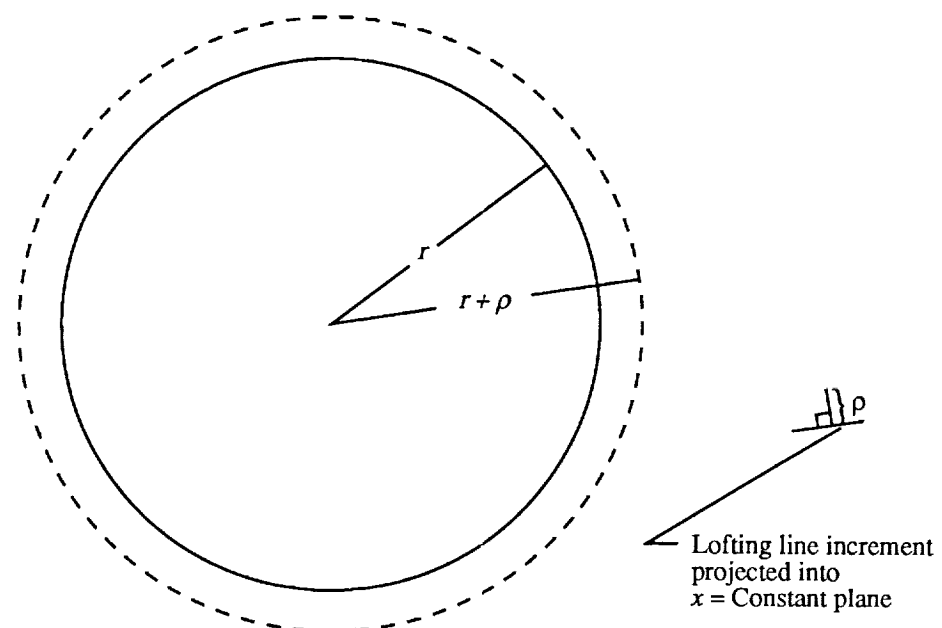
(a) Upper surface.

Figure 7. Example of computed fillet.

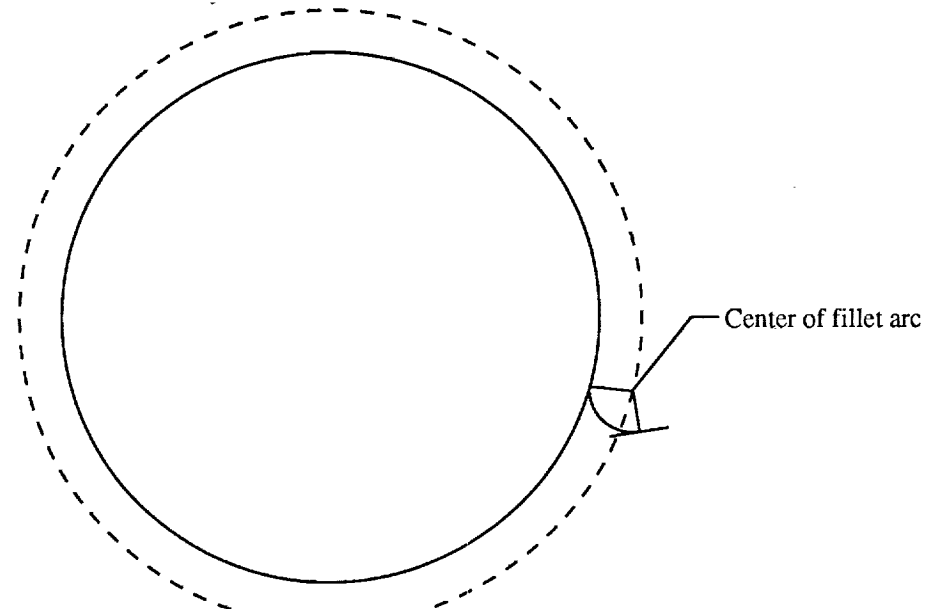


(b) Lower surface.

Figure 7. Concluded.



(a) Quantities used in iterative procedure.



(b) Converged solution.

Figure 8. System for inserting circular-arc fillet line.

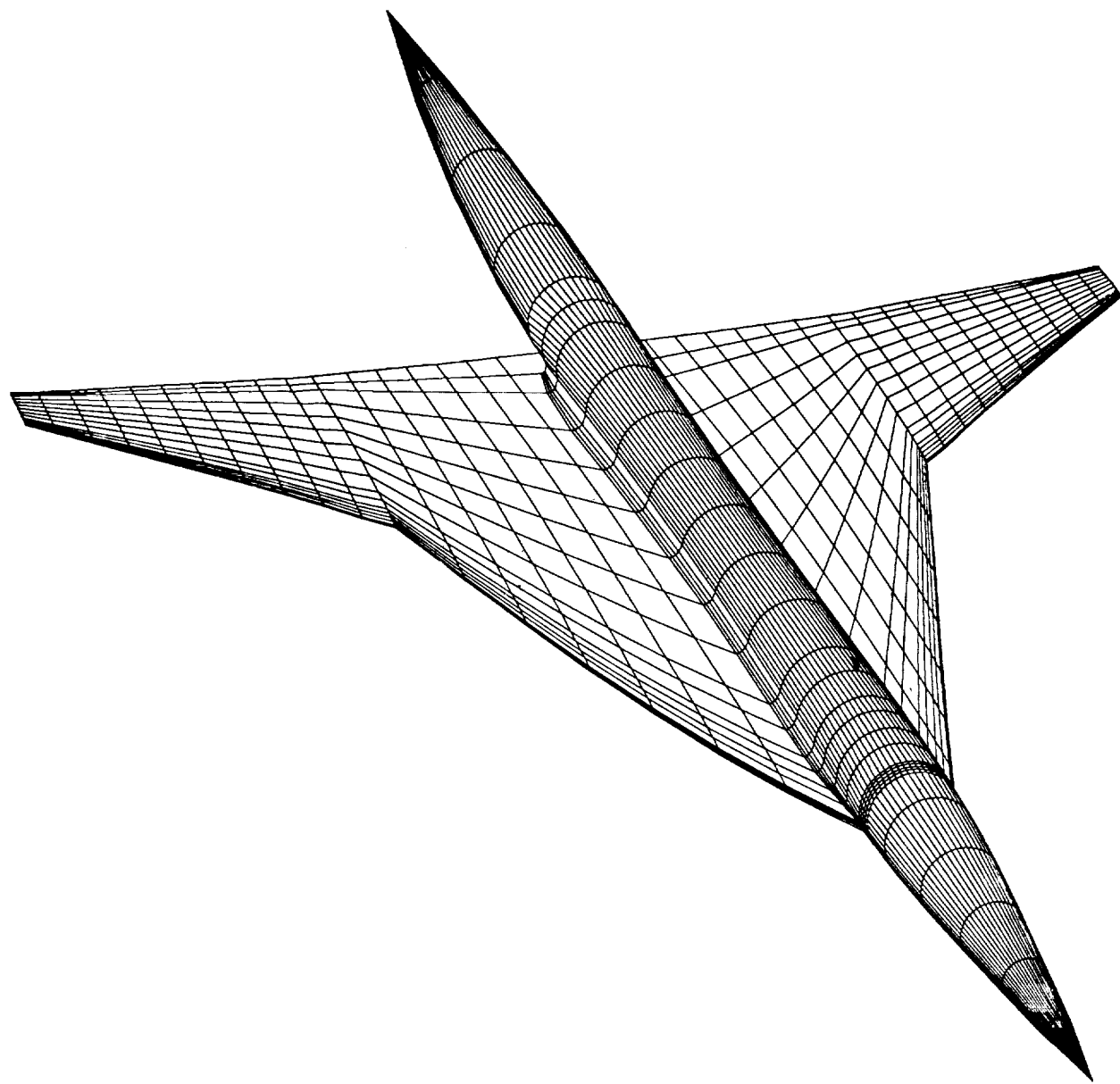


Figure 9. Example of computed circular-arc fillet.

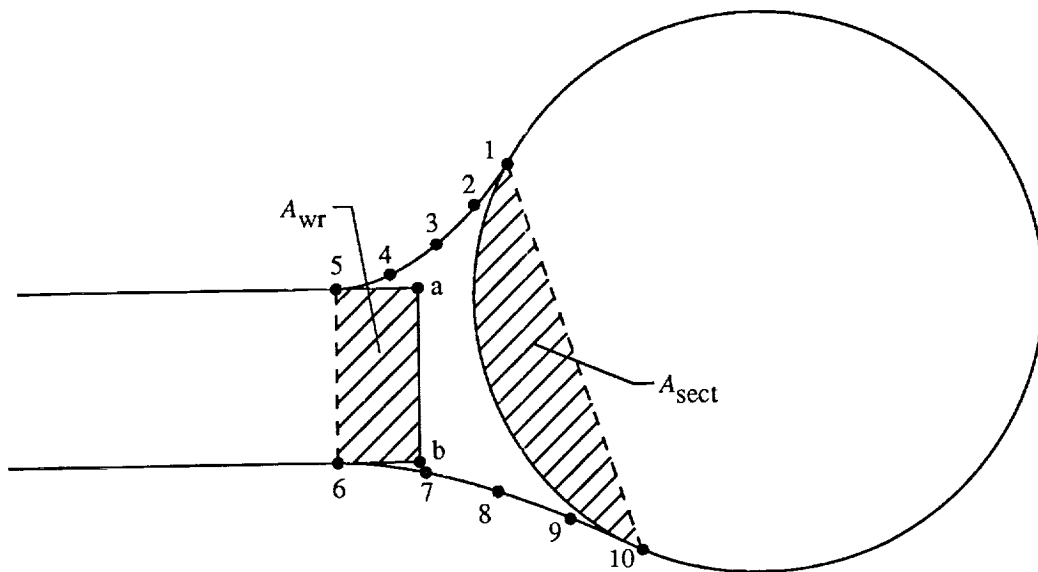


Figure 10. System for computing additional area due to fillet. Polygon vertices are marked by points 1 to 10.

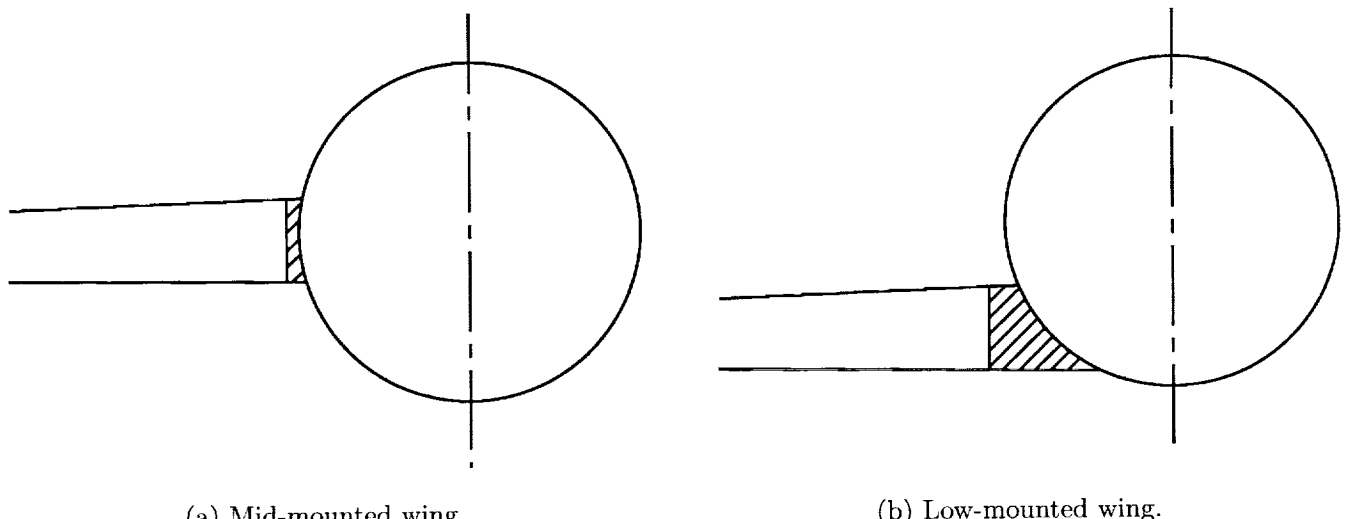


Figure 11. Diagrammatic comparison of added areas for mid-mounted and low-mounted wings (for computed intersection lines with no filleting).



REPORT DOCUMENTATION PAGE			Form Approved OMB No. 0704-0188
<p>Public reporting burden for this collection of information is estimated to average 1 hour per response, including the time for reviewing instructions, searching existing data sources, gathering and maintaining the data needed, and completing and reviewing the collection of information. Send comments regarding this burden estimate or any other aspect of this collection of information, including suggestions for reducing this burden, to Washington Headquarters Services, Directorate for Information Operations and Reports, 1215 Jefferson Davis Highway, Suite 1204, Arlington, VA 22202-4302, and to the Office of Management and Budget, Paperwork Reduction Project (0704-0188), Washington, DC 20503.</p>			
1. AGENCY USE ONLY (Leave blank)	2. REPORT DATE	3. REPORT TYPE AND DATES COVERED	
	March 1993	Technical Memorandum	
4. TITLE AND SUBTITLE Automatic Computation of Wing-Fuselage Intersection Lines and Fillet Inserts With Fixed-Area Constraint		5. FUNDING NUMBERS WU 505-59-53-01	
6. AUTHOR(S) Raymond L. Barger and Mary S. Adams			
7. PERFORMING ORGANIZATION NAME(S) AND ADDRESS(ES) NASA Langley Research Center Hampton, VA 23681-0001		8. PERFORMING ORGANIZATION REPORT NUMBER L-17131	
9. SPONSORING/MONITORING AGENCY NAME(S) AND ADDRESS(ES) National Aeronautics and Space Administration Washington, DC 20546-0001		10. SPONSORING/MONITORING AGENCY REPORT NUMBER NASA TM-4406	
11. SUPPLEMENTARY NOTES			
12a. DISTRIBUTION/AVAILABILITY STATEMENT Unclassified - Unlimited Subject Category 02		12b. DISTRIBUTION CODE	
<p>13. ABSTRACT (Maximum 200 words)</p> <p>Procedures for automatic computation of wing-fuselage juncture geometry are described. These procedures begin with a geometry in wave-drag format. First, an intersection line is computed by extrapolating the wing to the fuselage. Then two types of filleting procedures are described, both of which utilize a combination of analytical and numerical techniques appropriate for automatic calculation. An analytical technique for estimating the added volume due to the fillet is derived, and an iterative procedure for revising the fuselage to compensate for this additional volume is given. Sample results are included in graphical form.</p>			
14. SUBJECT TERMS Supersonic design; Surface geometry; Wing-body intersection; Fillet		<p>15. NUMBER OF PAGES 17</p> <p>16. PRICE CODE A03</p>	
17. SECURITY CLASSIFICATION OF REPORT Unclassified	18. SECURITY CLASSIFICATION OF THIS PAGE Unclassified	19. SECURITY CLASSIFICATION OF ABSTRACT	20. LIMITATION OF ABSTRACT